Synthesis of elastomeric polypropylene in bulk using C_1-symmetric *ansa*-metallocenes. New aspects of the synthesis of 1-(fluoren-9-yl)-2-(2-methyl-5,6-dihydrocyclopenta[*f*]-1*H*-inden-1-yl)ethane and complexes of zirconium and hafnium with this ligand

P. M. Nedorezova,[a]★ E. N. Veksler,[a] E. S. Novikova,[a] V. A. Optov,[a] A. O. Baranov,[a] A. M. Aladyshev,[a] V. I. Tsvetkova,[a] B. F. Shklyaruk,[b] D. P. Krut´ko,[c] A. V. Churakov,[d] L. G. Kuz´mina,[d] and J. A. K. Howard[e]

[a]*N. N. Semenov Institute of Chemical Physics, Russian Academy of Sciences, 4 ul. Kosygina, 119991 Moscow, Russian Federation. Fax: +7 (095) 137 8284. E-mail: pned@chph.ras.ru*

[b]*A. V. Topchiev Institute of Petrochemical Synthesis, Russian Academy of Sciences, 29 Leninsky prosp., 119991 Moscow, Russian Federation. Fax: +7 (095) 955 2224*

[c]*Department of Chemistry, M. V. Lomonosov Moscow State University, 1 Leninskie Gory, 119992 Moscow, Russian Federation. Fax: +7 (095) 932 8846. E-mail: kdp@org.chem.msu.su*

[d]*N. S. Kurnakov Institute of General and Inorganic Chemistry, Russian Academy of Sciences, 31 Leninsky prosp., 119991 Moscow, Russian Federation. Fax: +7 (095) 954 1279. E-mail: churakov@igic.ras.ru*

[e]*Department of Chemistry, University of Durham, South Road, Durham DH1 3LE, UK. Fax: +44 (0191) 384 4737. E-mail: j.a.k.howard@durham.ac.uk*

Isomeric 1-(fluoren-9-yl)-2-(2-methyl-5,6-dihydrocyclopenta[*f*]-1*H*-indenyl)ethanes **1a,b** and C_1-symmetric metallocenes, *viz.*, *rac*-{1-(η^5-fluoren-9-yl)-2-(2-methyl-5,6-dihydrocyclopenta[*f*]-η^5-inden-1-yl)ethane}zirconium dichloride (**9**) and *rac*-{1-(η^5-fluoren-9-yl)-2-(2-methyl-5,6-dihydrocyclopenta[*f*]-η^5-inden-1-yl)ethane}hafnium dichloride (**10**), with these ligands were synthesized by modified procedures. The structures of compounds **1b** (two crystalline modifications) and **10** were established by X-ray diffraction analysis. The synthesis of polypropylene (PP) in bulk was studied in the presence of polymethylalumoxane-activated metallocenes **9** and **10** in the temperature range of 30—70 °C. It was demonstrated that triisobutylaluminum can be used as a cocatalyst. In this case, the molecular weight of PP increases by a factor of ~2. An increase in the reaction temperature leads to an increase in stereoregularity and crystallinity of PP. The polymer synthesized at high temperatures crystallizes in the γ form. The resulting PP is characterized by a wide range of properties from rigid crystalline thermoplastic to amorphous elastomeric. Samples, which have a high molecular weight and moderate isotacticity, exhibit high elastomeric and durability properties.

Key words: zirconium, hafnium, C_1-symmetric *ansa*-metallocenes, X-ray diffraction analysis, propene polymerization, elastomeric polypropylene, microstructure, phase state.

The design of highly efficient homogeneous systems based on Group IV metal sandwich complexes opened up new possibilities for extending the grade range and fields of application of materials based on homo- and copolymers of α-olefins.[1—4] Due to the presence of active centers of the same type, these catalysts give a possibility to prepare polymers with a narrow molecular-weight distribution and compositionally homogeneous copolymers. The stereospecificity of the reactions can be varied as desired and polyolefins with different microstructures can be prepared by varying the composition, structure, and symmetry type of metallocenes. Catalytic systems based on these complexes offer wide possibilities to prepare new polymeric materials with unique properties, in particular, elastomeric polypropylene (PP).

Elastomeric PP, whose molecules consist of alternating stereoregular and random blocks, has been prepared for the first time[5] as a low-molecular-weight by-product

Published in Russian in *Izvestiya Akademii Nauk. Seriya Khimicheskaya,* No. 2, pp. 392—404, February, 2005.

1066-5285/05/5402-0400

in the synthesis of isotactic PP using heterogeneous catalytic systems. The discovery of metallocene catalysts, which ensure the formation of elastomeric PP as the major product in high yield, has inspired new interest in the synthesis of this polymer.

Several types of homogeneous metallocene catalysts proved to be efficient in the synthesis of elastomeric PP: (1) bis-indenyl 2-aryl-substituted complexes;[6,7] (2) "hybrid" systems involving simultaneously several types of metallocenes;[8,9] (3) C_1-symmetric *ansa*-metallocenes.[10—13]

Of particular interest is the examination of the possibility of synthesizing elastomeric PP with the use of C_1-symmetric *ansa*-metallocenes. Earlier,[12,13] several such complexes have been synthesized and the most active complexes have been revealed. The scheme of polymer chain growth, which has been described for the first time in the publication,[14] was used as the basis for the mechanism of action of C_1-symmetric metallocenes.[15] This mechanism assumes the presence of two centers with different stereospecificity and the competition between the chain growth and chain migration without monomer insertion. In this case, the polymer chain growth should lead to alternation of short isotactic sequences separated by single stereo defects.

The aim of the present study was to examine the effects of the nature of metal in the C_1-symmetric complexes, the modes of their activation, and the conditions of propene polymerization in bulk on the catalytic activity, microstructure, heat-transfer, and mechanical properties of the polymers. We also carried out a thorough study of 1-(fluoren-9-yl)-2-(2-methyl-5,6-dihydrocyclopenta[*f*]-1*H*-indenyl)ethanes **1a,b** serving as ligands, investigated the structures of intermediates formed in each step, and established the crystal structures of compound **1b** and the hafnium sandwich derived from **1b**.

Results and Discussion

Synthesis of 1-(fluoren-9-yl)-2-(2-methyl-5,6-dihydrocyclopenta[*f*]-1*H*-inden-1-yl)ethane (1b). Bis-cyclopentadienyl ligand **1b** was prepared according to a known procedure[15] presented in Scheme 1.

The drawback of this method is that the synthesis of the starting triflate **3** requires the use of expensive trifluoromethanesulfonic anhydride. We attempted to perform this reaction with the use of tosylate **6** instead of compound **3**. However, the reaction mixture contained (^{1}H NMR spectroscopic data) target products **1a,b** along with spiro compound **7**, the starting indene **4**, and other unidentifiable compounds in comparable amounts (Scheme 2, method *1*).

We succeeded in separating the reaction mixture by silica gel column chromatography and isolating all main products (**4**, **1a**, and **7**) in pure form. The total yield of compounds **1a** and **7** was 49%. In our opinion, the formation of spiro compound **7** is attributable to deprotonation of tosylate **6** with lithium salt **5** as the side reaction followed by intramolecular nucleophilic substitution. It should be noted that the reaction with compound **3** (see Ref. 15) did not afford by-product **7**, which may be associated with a considerable increase in the rate of nucleophilic substitution in going from tosylate **6** to triflate **3**.

Interestingly, the ligand prepared by the method *1* was isolated as isomer **1a** (the amount of isomer **1b** was $\leq$5%; ^{1}H NMR spectroscopic data). This can be explained as follows. Initially, the reaction affords isomer **1b**, which can, apparently, be deprotonated at the indenyl ring with

Scheme 1

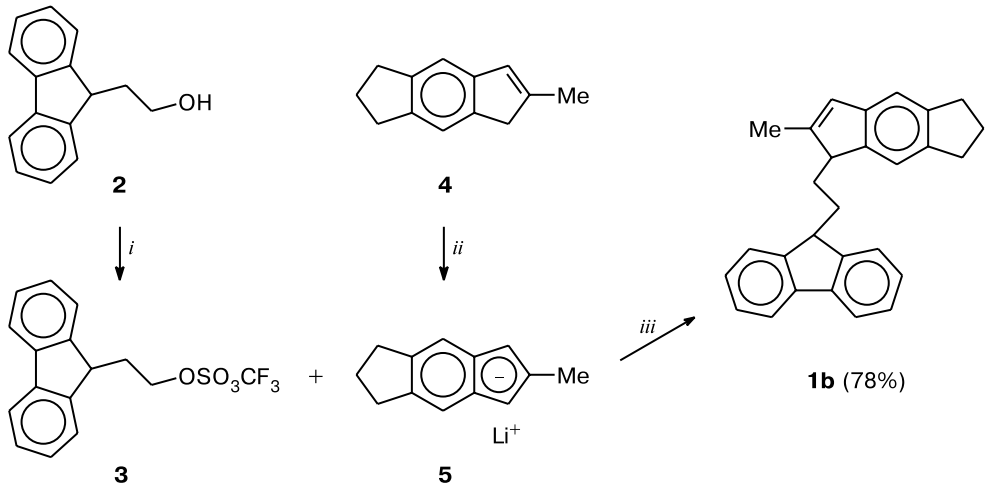

Reagent and conditions: *i*. $(CF_3SO_2)_2O$, CH_2Cl_2, Py, 0 °C. *ii*. BuLi, dioxane, 0 °C. *iii*. THF, 20 °C.

Scheme 2

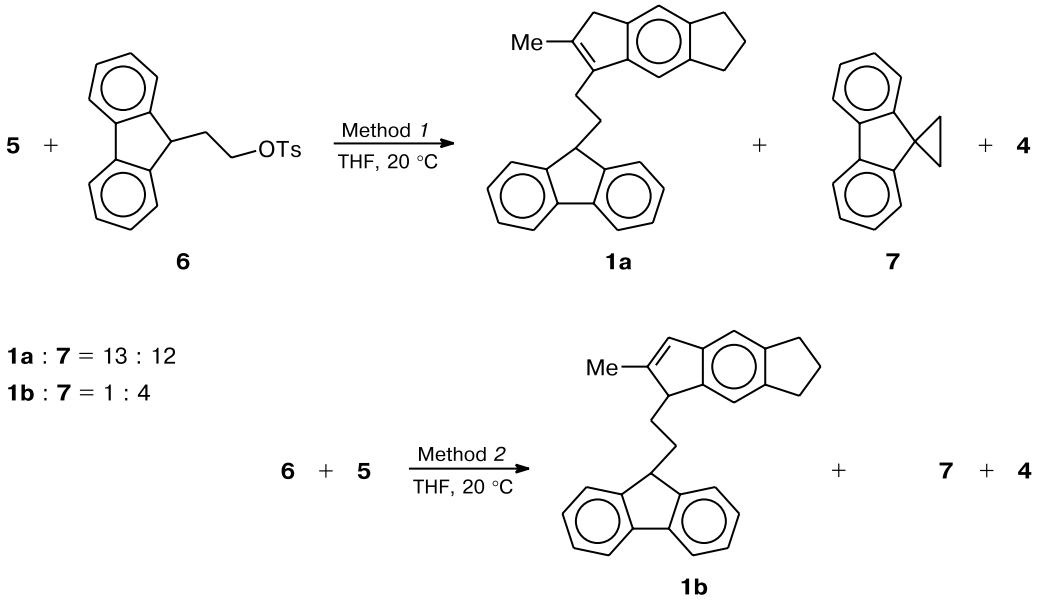

an excess of lithium salt **5** present in the solution to form the anion. The latter gives the target ligand as the thermodynamically most stable isomer **1a** upon quenching of the reaction mixture. It should be noted that isomer **1b** has been isolated earlier[15] under analogous conditions (the addition of triflate **3** to a solution of salt **5**; see Scheme 1).

With the aim of preventing side processes, which occur in the reaction mixture in the presence of an excess of anion **5**, we attempted to perform this reaction by mixing reagents in the reverse order (see Scheme 2, method *2*). As expected, the percentage of unidentifiable products in the mixture decreased substantially. The total yield of compounds **1b** and **7** was 80%. However, the ratio of these compounds changed in an undesirable way (see Scheme 2). In our opinion, an increase in the percentage of spiro compound **7** in the reaction mixture can be explained as follows. In this case, several competitive processes can occur at different rates. The initial step of the reaction involves slow nucleophilic substitution giving rise to the target product **1b** along with fast deprotonation of tosylate **6** with lithium salt **5**. The further intramolecular nucleophilic substitution affords product **7**. In these systems, deprotonation occurs much more rapidly than nucleophilic substitution. Therefore, in the initial step of the synthesis according to the method *2*, the concentration of tosylate **6** is substantially higher than that of lithium salt **5**, and the latter is virtually completely consumed for deprotonation of compound **6**, resulting in an undesirable change in the ratio of products **1** and **7** compared to the method *1*.

Therefore, the use of cheaper but less reactive tosylate **6** instead of triflate **3** led to a substantial decrease in the yield of the target products **1a,b** due to the side reaction giving rise to spiro compound **7**. Under particular conditions, the latter process becomes the major reaction (see Scheme 2, method *2*). Nevertheless, in spite of relatively low yields, we isolated isomers **1a** and **1b** in pure form (white crystalline compounds). Their structures were unambiguously established by ^{1}H and ^{13}C NMR spectroscopy. Earlier,[15] compound **1b** has been described as a yellow oil.

X-ray diffraction study of compound 1b. The molecular structures of two crystalline modifications of isomer **1b** were established by X-ray diffraction. One modification (monoclinic, space group $P2_1/c$) was prepared by slow crystallization from CH_2Cl_2, and another modification (orthorhombic, space group *Pbca*) was obtained by crystallization from the mother liquor during isolation of ligand **1** (a benzene—hexane—CH_2Cl_2 solvent mixture). The molecular structure of the monoclinic modification of **1b** is shown in Fig. 1. The bond lengths and bond angles for both modifications are given in Table 1. The structure of the monoclinic modification of **1b** consists of crystallographically equivalent molecules. The fluorenyl fragment is planar within 0.029(2) Å. The coordination environment of the fluorenyl C(1) atom is nearly tetrahedral (see Table 1). The C(14)—C(15) bond has an antiperiplanar conformation (the C(1)—C(14)—C(15)—C(16) torsion angle is 170.5(1)°). The exocyclic angles at the C(16)=C(17) double bond are smaller (~10°) than the endocyclic angles due to the geometric requirements of the C(16)—C(17)—C(18)—C(19)—C(27) five-membered ring. All C—C bond lengths in molecule **1b** have standard values tabulated for the corresponding bond types in organic compounds.[16]

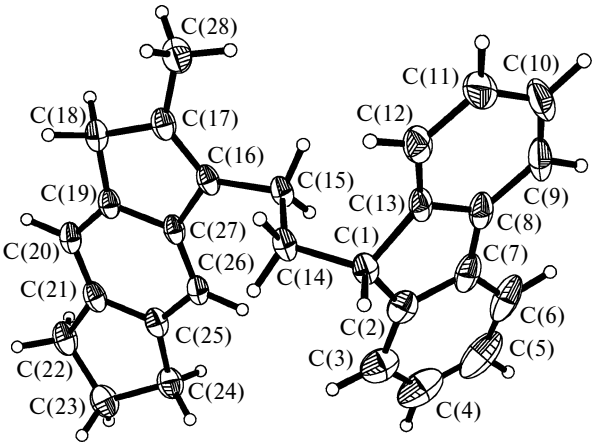

Fig. 1. Molecular structure of compound **1b** (the monoclinic modification, space group $P2_1/c$).

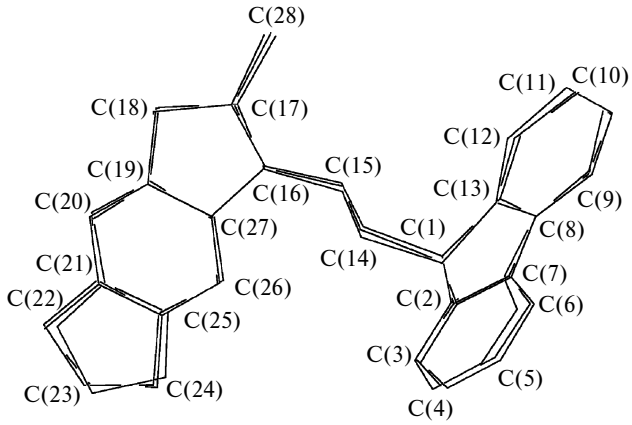

Fig. 2. Orthogonal superposition of molecule **1b** (the monoclinic modification, space group $P2_1/c$) and two crystallographically independent molecules **1b** (the orthorhombic modification, space group *Pbca*).

There are two crystallographically independent molecules in the structure of the orthorhombic modification of **1b**. On the whole, the geometric parameters (bond lengths, bond angles, and torsion angles) of both molecules **1b** in the orthorhombic modification and molecule **1b** in the monoclinic modification have very similar values (see Table 2). This is clearly seen from the results of the orthogonal superposition of these three molecules based on the coordinates of all nonhydrogen atoms (Fig. 2).

Synthesis of zirconium and hafnium complexes was carried out according to a known procedure,[15] which was slightly improved. Deprotonation of ligand **1** with Bu^nLi in diethyl ether afforded dilithium salt **8** in virtually quantitative yield, and this reaction product was characterized by ^1H and ^{13}C NMR spectroscopy (Scheme 3). The reaction of salt **8** with $ZrCl_4$ or $HfCl_4$ in toluene produced the corresponding *ansa*-complexes **9** and **10** in high yields. The resulting metallocenes were characterized by ^1H and ^{13}C NMR spectroscopy. The structure of the hafnium complex was established by X-ray diffraction.

Single crystals of complex **10** were prepared by slow crystallization from CH_2Cl_2. The molecular structure of compound **10** is shown in Fig. 3. The bond lengths and bond angles are given in Table 2. On the whole, the geometric parameters of molecule **10** are similar to those found earlier[15] for isostructural zirconium analog **9**. In the hafnium complex, the metal—ligand bonds are slightly shorter than those in the zirconium complex, whereas the bond angles remain virtually unchanged (see Table 2).

Propene polymerization in the presence of catalysts based on complexes 9 and 10. Data on the catalytic activity of systems based on complexes **9** and **10** activated with polymethylalumoxane (MAO) and selected properties of the resulting PP are given in Table 3. The MAO concentration was 0.46—1.1 g L^{-1}. As the polymerization tem-

Table 1. Selected bond lengths (d) and bond angles (ω) in molecules **1b** (space groups $P2_1/c$ and *Pbca*)

Bond	d/Å			Angle	ω/deg		
	$P2_1/c$	*Pbca**			$P2_1/c$	*Pbca**	
		I	II			I	II
C(1)—C(2)	1.515(2)	1.505(8)	1.502(8)	C(13)—C(1)—C(14)	115.2(1)	113.6(5)	115.6(5)
C(1)—C(13)	1.518(2)	1.508(8)	1.503(7)	C(2)—C(1)—C(14)	114.5(1)	116.5(5)	114.6(5)
C(1)—C(14)	1.539(2)	1.533(6)	1.531(6)	C(1)—C(14)—C(15)	113.0(1)	115.0(4)	113.0(4)
C(14)—C(15)	1.540(2)	1.514(6)	1.531(6)	C(14)—C(15)—C(16)	112.2(1)	112.9(4)	113.7(4)
C(15)—C(16)	1.502(2)	1.499(6)	1.492(6)	C(15)—C(16)—C(17)	128.2(1)	127.0(6)	129.1(6)
C(16)—C(17)	1.356(2)	1.336(7)	1.342(7)	C(15)—C(16)—C(27)	122.6(1)	123.2(6)	121.7(6)
C(16)—C(27)	1.469(2)	1.441(7)	1.492(7)	C(16)—C(17)—C(28)	127.6(1)	129.2(6)	128.0(6)
C(17)—C(18)	1.514(2)	1.512(6)	1.511(7)	C(16)—C(17)—C(18)	110.5(1)	109.3(5)	110.0(6)
C(17)—C(28)	1.496(2)	1.490(7)	1.474(7)	C(18)—C(17)—C(28)	121.9(1)	121.5(5)	121.9(5)
C(18)—C(19)	1.506(2)	1.495(6)	1.499(6)	C(17)—C(18)—C(19)	103.4(1)	103.7(5)	103.8(5)

* Two independent molecules I and II.

Scheme 3

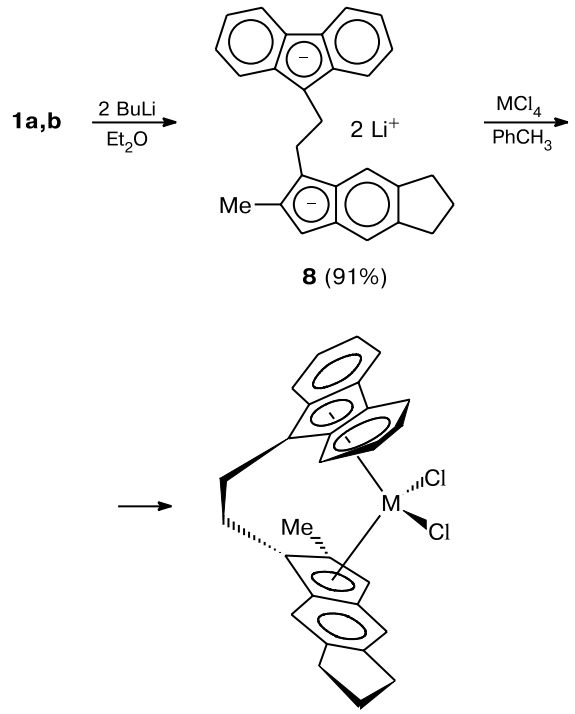

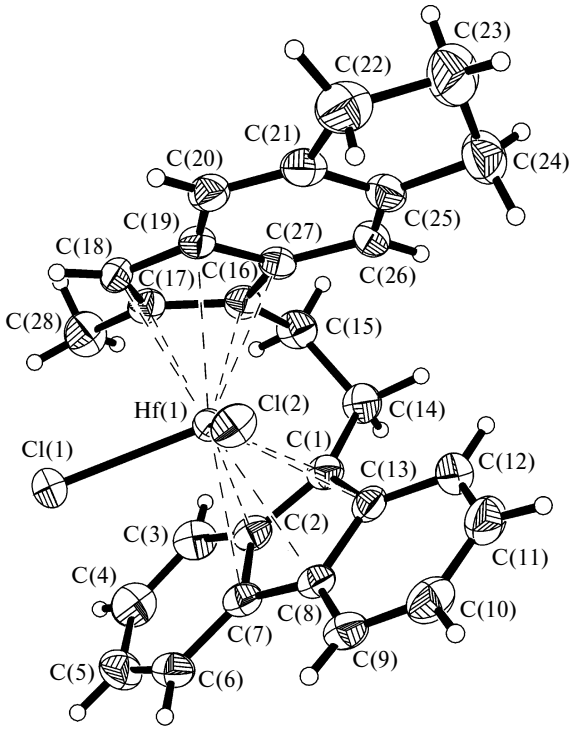

Fig. 3. Molecular structure of compound **10**.

Table 2. Selected bond lengths (*d*) and bond angles (ω) in molecule **10**

Bond	*d*/Å
Hf(1)—Cl(2)	2.384(2)
Hf(1)—Cl(1)	2.401(1)
C(1)—C(14)	1.514(5)
C(14)—C(15)	1.522(6)
C(15)—C(16)	1.495(5)
Hf(1)—Flu*	2.252
Hf(1)—Ind**	2.203
Angle	**ω/deg**
Cl(2)—Hf(1)—Cl(1)	97.03(5)
C(1)—C(14)—C(15)	111.9(3)
C(16)—C(15)—C(14)	111.8(3)
Flu*—Hf(1)—Ind**	129.0
C(1)—C(14)—C(15)—C(16)	36.2(5)

* Flu is the center of the η^5 ring of fluorene.
** Ind is the center of the η^5 ring of indene.

perature increases from 30 to 70 °C, the yield of PP increases and reaches 104 (kg PP) (mmol Zr)$^{-1}$ h^{-1} for the **9**—MAO system and 14 (kg PP) (mmol Hf)$^{-1}$ h^{-1} for the **10**—MAO system (see Table 3). The activity of the catalytic system based on complex **10** is lower than that of the system based on complex **9** throughout the temperature range. A decrease in the polymerization rate in the reactions with the use of hafnocenes is generally accompanied by a substantial increase in the molecular weight of the polymers. The smaller size of the Hf atom and an increase in the charge on this atom lead to metal—carbon bond strengthening,[17] generally resulting in a decrease in the reaction rates of the monomer insertion and limitation of the polymer chain growth due to β-hydride elimination.[18]

The kinetic curves of propene polymerization in the presence of the **9**—MAO and **10**—MAO catalytic systems are shown in Fig. 4. For both catalytic systems, the maximum activity is observed at the initial instant of time followed by a decrease in the polymerization rate. The activation energies of polymerization in the presence of the **9**—MAO and **10**—MAO catalytic systems were estimated from the maximum observed polymerization rates. These energies are 11.4 and 16.9 kcal mol^{-1}, respectively.

An increase in the polymerization temperature leads to an increase in regularity of the polymers (see Table 3). For the **9**—MAO system at high concentrations of the monomer (10—12 mol L^{-1}), the regularity gradually increases with increasing temperature. At low concentrations of the monomer (1.1 mol L^{-1}), the regularity of PP reaches the maximum observed value already at 50 °C.[15]

It should be noted that, unlike metallocenes with the symmetry C_2 [19,20] and C_s,[21,22] C_1-symmetric metallocenes are characterized by an increase in the degree of isotacticity

Table 3. Propene bulk polymerization in the presence of the **9**—MAO and **10**—MAO catalytic systems

Run	Complex	T/°C	[M]·10^{-6} /mol	Al : M[a]	[MAO] /g L^{-1}	t[b] /min	Yield /g	Activity[c]	D_{998}/D_{973}	M.p. /°C
1	**9**	30	1.66	3800	0.9	45	26.3	21.1	0.25	—
2	**9**	50	1.00	4480	0.65	120	50.0	25.0	0.33	123
3	**9**	70	0.63	5064	0.5	30	33.0	104.0	0.58	120
4	**10**	30	2.94	2602	1.1	180	13.0	1.5	0.26	—
5	**10**	50	1.73	4090	1.0	120	21.0	6.0	0.42	53—76
6	**10**	70	1.28	4250	0.8	60	35.0	14.0	0.45	55—87

[a] M = Zr, Hf; molar ratio.
[b] Polymerization time.
[c] In (kg PP) (mmol M)$^{-1}$ h^{-1}.

of PP with increasing polymerization temperature. These changes become clear from the scheme of the polypropylene synthesis in the presence of C_1-symmetric metallocenes.[15] An increase in the reaction temperature and a decrease in the concentration of the monomer promote an increase in the rate of chain migration without monomer insertion and, correspondingly, an increase in the amount of isotactic pentads. To the contrary, an increase in the concentration of the monomer increases the probability of the insertion of the monomer at a nonselective coordination vacancy, resulting in a decrease in isotacticity.[15] It should be noted that an increase in the monomer concentration in the PP synthesis with the use of C_2- and C_s-symmetric metallocenes facilitates an increase in regularity of PP due to a relative decrease in the rates of the processes producing stereo- and regioerrors in the polymer chain.[19—21]

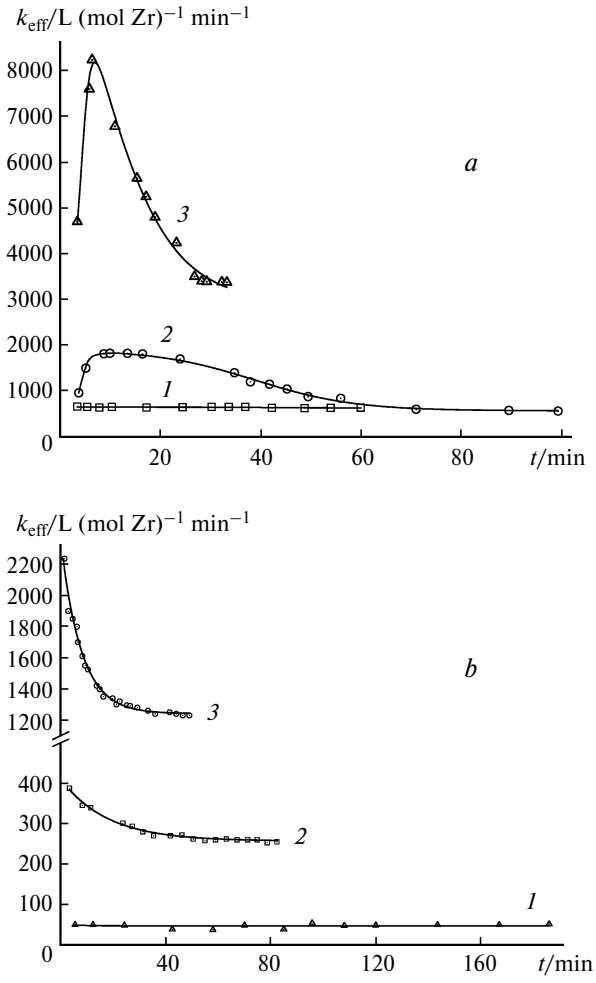

Fig. 4. Kinetic curves of propene bulk polymerization in the presence of the **9**—MAO (*a*) and **10**—MAO (*b*) catalytic systems at polymerization temperatures of 30 (*1*), 50 (*2*), and 70 °C (*3*). For the polymerization conditions, see Table 3.

The formation of single stereo defects giving rise to mrrm sequences in the polymer chain, is generally confirmed by the fact that the mmmr : mmrr : mrrm pentad ratio is 2 : 2 : 1. The data on the stereo composition of PP prepared at 70 °C in the presence of MAO-activated complexes **9** and **10** are given in Table 4. It can be seen that these pentad contents are satisfactorily described by this ratio.

We examined the possibility to partially replace MAO with triisobutylaluminum (TIBA). A need to search for alternative cocatalysts is associated primarily with a high cost of MAO and the necessity of using large excesses of MAO. Earlier,[22,23] it has been demonstrated that

Table 4. Pentad composition of polypropylene prepared in the presence of the **9**—MAO and **10**—MAO catalytic systems at 70 °C

Composition	Run *3*	Run *6*
mmmm	47.16	43.30
mmmr	13.41	15.54
rmmr	3.26	2.40
mmrr	13.66	14.44
rmrr + mmrm	4.76	4.66
mrmr	3.52	4.70
rrrr	2.35	2.18
mrrr	4.04	4.25
mrrm	7.15	7.41

Table 5. Propene bulk polymerization with the use of the catalytic systems based on TIBA-activated complexes **9** and **10** (polymerization temperature was 50 °C)

Run	Complex	[M]·10^{-6} /mol	Al(MAO)/M[a]	Al(TIBA)/M[a]	Al(TIBA)/Al(MAO)	[TIBA] /g L^{-1}	t[b] /min	Yield /g	Activity[c]	D_{998}/D_{973}
2	**9**	1.0	4480	—	—	—	120	50	25	0.33
5	**10**	1.73	4090	—	—	—	120	21.0	6.0	0.42
7	**9**	0.79	300	1865	6.1	0.7	65	12	14	0.25
8	**9**	1.53	300	1047	3.4	0.7	60	40	27	0.25
9	**9**	1.27	300	753	2.5	0.45	60	36	28	0.22
10	**9**	2.50	300	223	0.7	0.26	40	50	30	0.36
11	**10**	2.56	320	550	1.7	0.6	120	0.22	0.043	0.33

[a] M = Zr, Hf; molar ratio.
[b] Polymerization time.
[c] In (kg PP) (mmol M)$^{-1}$ h^{-1}.

dimethyl derivatives of 2,2′-disubstituted bis-indenyl zirconocenes can be successfully activated with TIBA, the change in the TIBA : metallocene ratio influencing substantially both the stereoregularity and molecular weight of the resulting polymers. We suggested that TIBA can be used as a cocatalyst for complexes **9** and **10** predissolved in small amounts of MAO, which is required for the formation of dimethyl derivatives. The results of propene polymerization in the presence of the combined cocatalysts are given in Table 5 and presented in Fig. 5. The Al(TIBA) : Zr molar ratio was measured in a wide range from 1860 to 220. At high Al(TIBA) : Zr ratios, the system exhibits the highest activity at the initial instant of time, after which sharp deactivation occurs (see Fig. 5). A decrease in the Al(TIBA) : Zr ratio leads to a decrease in the initial activity; however, the catalytic system is more stable. The yield of PP became comparable with that obtained in the reaction with the use of polymethylalumoxane-activated complex **9** in the absence of a TIBA additive. In the presence of the latter as a cocatalyst, the concentration of the organoaluminum compound can be decreased to 0.26 g L^{-1} without a loss of activity (see Table 5, run *10*).

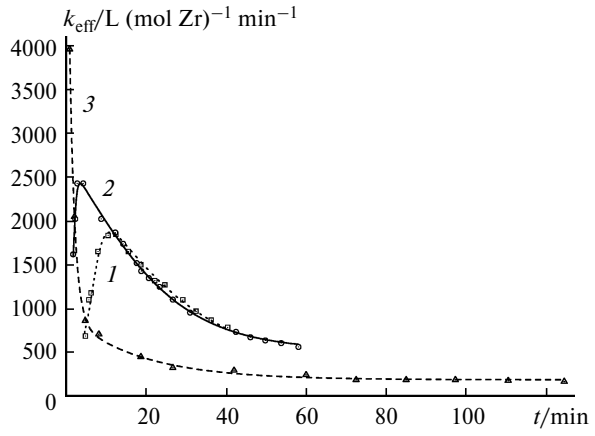

Fig. 5. Kinetic curves of propene bulk polymerization with the use of the **9**—TIBA—MAO catalytic system: Al(TIBA) : Zr = 1700 (*1*), 700 (*2*), and 220 (*3*). The polymerization temperature was 50 °C. For the polymerization conditions, see Table 5.

The stereoregularity of the polypropylene synthesized depends on the Al(TIBA) : Zr ratio (see Table 5). For the Al(TIBA) : Zr ratios varying from 750 to 1860, the regularity of the chain is smaller than that of PP prepared in the presence of the **9**—MAO system, whereas a further decrease in this ratio to 220 leads to the formation of a polymer characterized by higher stereoregularity. The results of our study provided evidence that TIBA influences the active centers of the catalytic complex. Most likely, at higher Al(TIBA) : Zr ratios, TIBA hinders the polymer chain migration without monomer insertion, resulting in a decrease in the regularity of PP. The use of complex **10** as the catalyst in the presence of TIBA leads to a sharp decrease in the catalytic activity (see Table 5). Presumably, steric hindrances resulting from interactions of complex **10** with the bulky isobutyl fragments of TIBA hinder the insertion of the propylene molecule into the polymer chain.

The molecular weights of the polymers, which were synthesized at 50 °C in the presence of the **9**—MAO, **10**—MAO, and **9**—MAO—TIBA catalytic systems, are given in Table 6 (samples were synthesized in runs *2*, *5*, and *8*, see Tables 3 and 5). As expected, the molecular

Table 6. Molecular-weight characteristics of the polymers synthesized with the use of catalytic systems based on complexes **9** and **10**

Run	Complex	$M_w \cdot 10^{-3}$	$M_n \cdot 10^{-3}$	M_w/M_n	$M_Z \cdot 10^{-3}$
2	**9**	146	76	1.9	240
5	**10**	177	96	1.8	277
8	**9**	294	131	2.2	540

Note. M_w, M_n, and M_Z are the weight-average, number-average, and Z-average molecular weights, respectively.

weights of the polymers synthesized with the use of the **10**—MAO catalytic system under identical polymerization conditions are higher than those preprared in the presence of the **9**—MAO system. It is particularly interesting that the molecular weight of PP prepared using activation with TIBA increases by a factor of ~2. These data indicate that TIBA inhibits reactions limiting the polymer chain growth and confirm that TIBA is involved in the active centers. Therefore, the use of TIBA as the cocatalyst allows one to vary the molecular-weight characteristics and microstructure of PP.

An analogous increase in the molecular weight of PP was observed also for propene bulk polymerization in the presence of the (2-PhInd)$_2$ZrMe$_2$—TIBA catalytic system compared to the (2-PhInd)$_2$ZrCl$_2$—MAO system (Ind is indenyl).[22,23] It should be noted that the combined cocatalyst has virtually no effect on the molecular weight of PP prepared in the presence of systems based on $Me_2SiInd_2ZrCl_2$ and $Ph_2C(Cp)(Flu)ZrCl_2$ (Flu is fluorenyl).[24,25]

We studied polymers, which were prepared under various polymerization conditions with the use of complexes **9** and **10**, by X-ray diffraction and examined the heat-transfer properties and the deformation behavior of the polymers.

X-ray diffraction patterns of PP obtained at different polymerization temperatures are given in Fig. 6, *a* and *b*. An increase in the reaction temperature results in the formation of PP, whose properties vary from those of a completely amorphous polymer (30 °C) to those of a polymer characterized by pronounced crystallinity peaks (70 °C). The degree of crystallinity of PP prepared with the use of both types of catalytic systems is as high as 30—37%. It can be seen that PP synthesized in the presence of complex **10** is characterized by more diffuse crystallinity peaks, which is evidence for a smaller size of crystallites. Interestingly, PP prepared at high temperatures crystallizes in the γ form. This fact is generally associated with the presence of a large number of stereo- and regioerrors in the polymer chain.[26]

We analyzed the crystal structures of the polymers synthesized with the use of the **9**—MAO and **10**—MAO catalytic systems in runs *3* and *6*. The results of our study were compared with analogous results obtained in the investigation of the γ form of isotactic PP with high crystallinity.[27,28] For the PP samples prepared in runs *3* and *6*, the *c* parameter characterizing the size of the unit cell of the crystallites along the *Z* axis is 42.45 and 42.20 Å, respectively. These values differ only slightly from those found earlier for the γ form of isotactic PP.[27,28] Presumably, the *c* parameter is independent of the degree of crystallinity of PP. The main difference is that crystallites of PP grow differently in different planes. The parameters of the structure are virtually equal along the 00*l* direction (L_{008} ~200 Å) and differ slightly from the corresponding

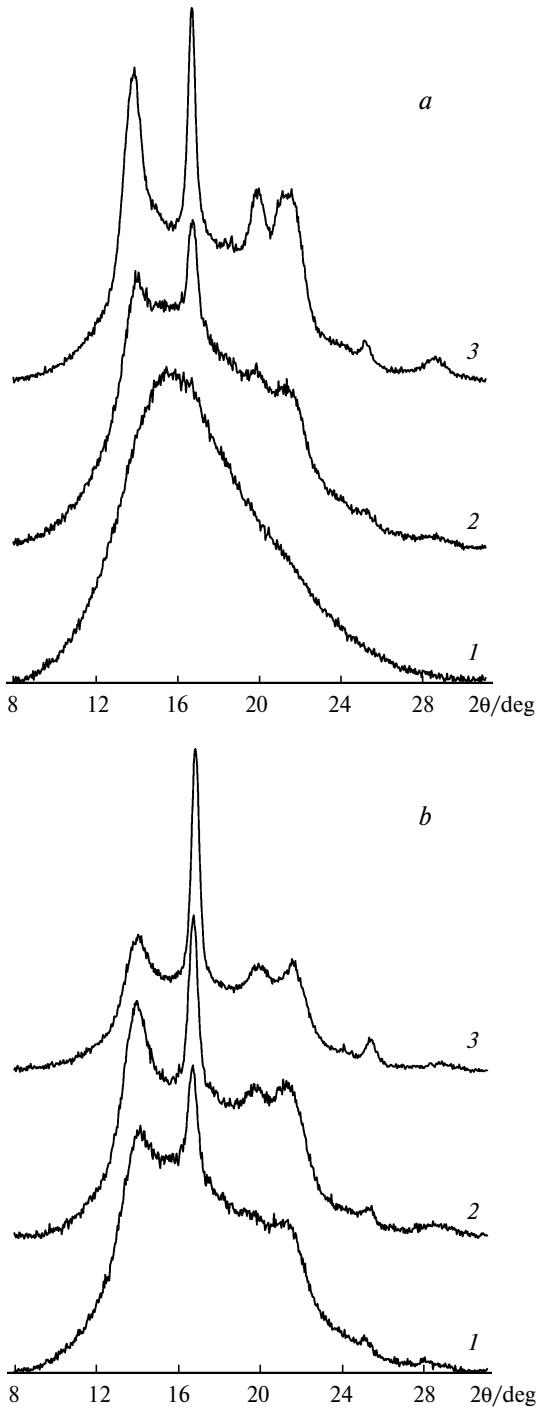

Fig. 6. X-ray diffraction patterns of PP prepared in the presence of the **9**—MAO (*a*) and **10**—MAO (*b*) catalytic systems at polymerization temperatures of 30 (*1*), 50 (*2*), and 70 °C (*3*).

values for the γ form of isotactic PP, which was prepared by crystallization of the polymer at high pressures,[28] whereas the sizes of the crystallites in other directions of the planes (L_{111}, L_{117}, L_{202}, L_{026}) are noticeably different. For example, L_{202} is 230 Å along the *h*0*l* direction,[28]

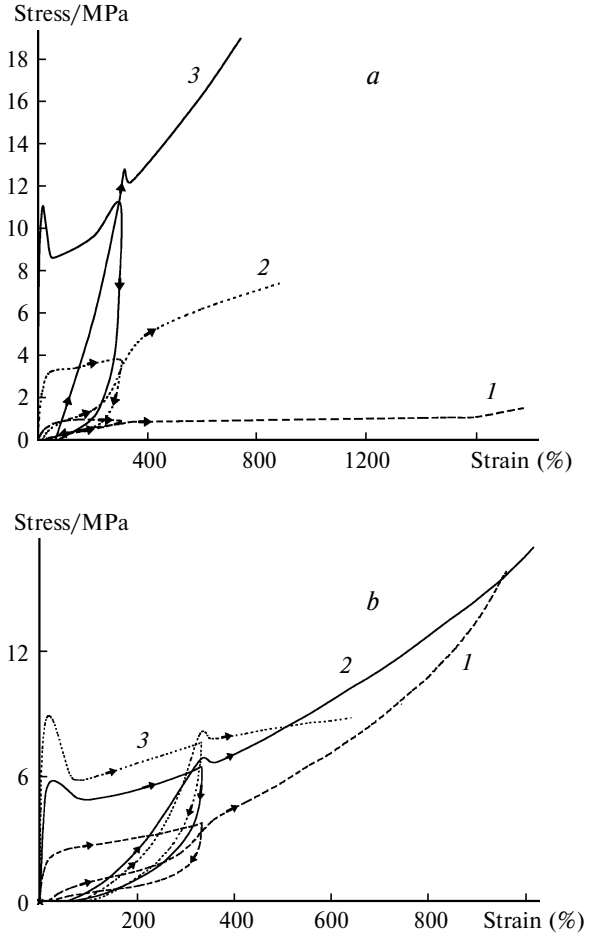

Fig. 7. Stress-strain curves of PP prepared in the presence of the **9**—MAO (*a*) and **10**—MAO catalytic systems (*b*) at polymerization temperatures of 30 (*1*), 50 (*2*), and 70 °C (*3*).

whereas this parameter in our samples changes to 113 Å (run *3*) and 85 Å (run *6*).

The melting points of the PP samples prepared in the presence of complex **9** (120—123 °C) are substantially higher than those of the samples synthesized with the use of complex **10** (60—80 °C) (see Table 3). The lower melting point of PP prepared in the presence of complex **10** and the character of X-ray diffraction patterns suggest that macromolecules of this polymer contain shorter isotactic sequences compared to PP synthesized in the presence of complex **9**.

The stress-strain curves of elastomeric PP and the hysteresis curves are shown in Fig. 7, *a* and *b*. The data on the stress-strain characteristics of the polymers are given in Table 7. It can be seen that more stereoregular PP samples with high crystallinity are characterized by higher strength, larger Young's moduli, and residual strain. Samples of PP prepared at 30 °C possess better elastomeric properties. For example, elastomeric PP synthesized in the presence of complex **9** is characterized by the largest strain (>1750%) and the residual strain ε_{300} of 20%. Elastomeric PP prepared in the presence of complex **10** has ε_{300} = 12%, and the residual strain after rupture is as low as 14%. Interestingly, this polymer can be reinforced during strain. In this case, the rupture stress is 16 MPa. The possibility of reinforcing is associated with the presence of small crystallizable propylene sequences in the polymer.

The samples of elastomeric PP synthesized in the presence of the combined MAO + TIBA cocatalyst (runs *8—10*) have a lower degree of crystallinity and higher elastomeric properties compared to the samples prepared under the same polymerization conditions with the use of only MAO as the cocatalyst (run *2*). The residual strain ε_{300} for the samples prepared in runs *8—10* varies in a range of 12.3—16.8%, whereas ε_{300} for the sample prepared in run *2* is 43% (see Table 7).

To summarize, we investigated the effects of the leaving group and the order in which the reagents are mixed on the yield of the target ligand in the synthesis of metallocenes **9** and **10** and determined the structures of by-products. The crystal structures of ligand **1b** and

Table 7. Stress-strain characteristics of polymers (the strain rate was 500 mm min^{-1})

Run	Complex	D_{998}/D_{973}	Crystallinity (%)	E	σ_r	ε_r	ε_{300}	ε_{res}
				MPa			%	
1	**9**	0.25	0	3.4	>1.5	>1750	19.8	—
2	**9**	0.33	18	21.6	9.12	884	43.2	51
3	**9**	0.58	36	324.0	19.1	735	62.7	487
4	**10**	0.25	16	31.7	16.0	865	12.0	14
5	**10**	0.42	29	84.7	17.2	916	38.1	115
6	**10**	0.45	36	187.0	8.9	577	67.8	473
8	**9**	0.25	13	12.5	11.6	1008	12.3	27
9	**9**	0.22	7	7.2	8.08	1000	10.8	26
10	**9**	0.36	17	18.4	10.0	863	16.8	54

Note. E is Young's modulus, σ_r is the rupture stress, ε_r is the rupture strain, ε_{300} is the residual strain, and ε_{res} is the residual stress measured for samples immediately after tests (related to the initial length of the sample).

hafnium sandwich **10** were established. Highly active PP with a controlled structure of the polymer chain can be synthesized by varying the structure of the metallocene catalyst, polymerization conditions, and the nature of the cocatalyst. The properties of the resulting PP vary from rigid thermoplastic to amorphous elastomeric. The use of TIBA instead of MAO holds more promise for the preparation of elastomeric PP.

Experimental

Metallocenes were synthesized under an atmosphere of high-purity argon or in evacuated all-sealed Schlenk-type vessels. The solvents were dried before use according to standard procedures.[29] Ethylene oxide was purified by drying over CaH_2 at −18 °C and twice freezing from CaH_2 under high vacuum. Commercial $ZrCl_4$, $HfCl_4$, $AlCl_3$, and indane (Aldrich) were used. Chlorides $ZrCl_4$ and $HfCl_4$ were additionally purified by sublimation in a stream of hydrogen at 330—350 °C. Methacrylic acid chloride was prepared by the reaction of methacrylic acid with an excess of PCl_3 and purified by fractional distillation.

The ^1H and ^{13}C NMR spectra were recorded on a Varian VXR-400 spectrometer (400 and 100 MHz, respectively) with the use of the signals of the residual protons and signals of the carbon atoms of the corresponding deuterated solvents, respectively, as the internal standards (δ_H 7.24 and δ_C 77.0 ($CDCl_3$), δ_H 5.32 and δ_C 53.8 (CD_2Cl_2), δ_H 1.73 and δ_C 25.3 (THF-d_8)). Elemental analysis was carried out on an automated Carlo-Erba analyzer.

2-(Fluoren-9-yl)ethanol (2) was prepared from fluorene (36.5 g, 214.0 mmol) according to a known procedure.[30] Compound **2** contained (^1H NMR spectroscopic data) ~15% of 9,9′-bis(2-hydroxyethyl)fluorene as an impurity. Repeated crystallization from a 2 : 3 toluene—light petroleum mixture did not lead to a change in the product ratio. The target compound was purified by column chromatography on silica gel (CH_2Cl_2 as the eluent). After removal of the solvent and high-vacuum drying, compound **2** was obtained as white crystals in a yield of 26.4 g (59%). ^1H NMR ($CDCl_3$, 25 °C), δ: 1.20 (br.s, 1 H, OH); 2.29 (q, 2 H, C$\underline{H}_2$CH$_2$OH, $^3J_{H,H}$ = 6.8 Hz); 3.58 (t, 2 H, C$\underline{H}_2$OH, $^3J_{H,H}$ = 6.8 Hz); 4.12 (t, 1 H, H(9), $^3J_{H,H}$ = 6.8 Hz); 7.27—7.38 (m, 4 H, H(2), H(3), H(6), H(7)); 7.53 and 7.75 (both d, 2 H each, H (1), H(4), H(5), H(8), $^3J_{H,H}$ = 8.0 Hz).

9,9′-Bis(2-hydroxyethyl)fluorene. ^1H NMR ($CDCl_3$, 25 °C), δ: 1.20 (br.s, 2 H, OH); 2.37 (t, 4 H, C$\underline{H}_2$CH$_2$OH, $^3J_{H,H}$ = 6.8 Hz); 2.99 (t, 4 H, C$\underline{H}_2$OH, $^3J_{H,H}$ = 6.8 Hz); 7.25—7.72 (m, 8 H, H arom.).

2-(Fluoren-9-yl)ethyl tosylate (6).[31] Tosyl chloride (17.2 g, 90.0 mmol) was added with stirring to a solution of alcohol **2** (19.0 g, 90.0 mmol) in pyridine (150 mL) at 0 °C. The reaction mixture was allowed to warm to ~20 °C, kept for ~18 h, and poured into ice water. The product was extracted with Et_2O (3×150 mL). The combined ethereal extracts were washed with dilute HCl until pH became weakly acidic and then with water and dried with $MgSO_4$. The solution was concentrated in vacuum created by a water-aspirator pump, and the precipitate was filtered off, washed on a filter with hexane, and dried under high vacuum. A white crystalline compound was obtained in a yield of 22.0 g (67%). ^1H NMR ($CDCl_3$, 25 °C), δ: 2.29 (q, 2 H, C$\underline{H}_2$CH$_2$O, $^3J_{H,H}$ = 6.6 Hz); 2.44 (s, 3 H, Me); 3.99 (t, 2 H, CH$_2$O, $^3J_{H,H}$ = 6.6 Hz); 4.04 (t, 1 H, H(9), $^3J_{H,H}$ = 6.6 Hz); 7.25 and 7.31 (both t, 2 H each, H(2), H(3), H(6), H(7), $^3J_{H,H}$ = 8.0 Hz); 7.35 and 7.70 (both m, 4 H each, H(1), H(4), H(5), H(8) and H arom. of tosyl). $^{13}C\{^1H\}$ NMR ($CDCl_3$, 25 °C), δ: 21.60 (Me); 32.29 (C$\underline{H}_2$CH$_2$OH); 43.62 (CH(9)); 67.71 (CH$_2$O); 119.98, 124.25, 127.05, 127.33, 127.85, 129.79 (CH arom.); 132.93, 144.71 (C arom. of tosyl); 140.83, 145.64 (C arom. of fluorene).

2-Methyl-5,6-dihydrocyclopenta[*f*]-1*H*-indene (4).[15] ^1H NMR ($CDCl_3$, 25 °C), δ: 2.11 (quint, 2 H, CH$_2$C$\underline{H}_2$CH$_2$, $^3J_{H,H}$ = 7.2 Hz); 2.16 (s, 3 H, Me); 2.93 (t, 4 H, C$\underline{H}_2$CH$_2$C$\underline{H}_2$, $^3J_{H,H}$ = 7.2 Hz); 3.26 (s, 2 H, CH$_2$ of indene); 6.46 (s, 1 H, =CH of indene); 7.13 and 7.25 (both s, 1 H each, H arom.). $^{13}C\{^1H\}$ NMR ($CDCl_3$, 25 °C), δ: 16.78 (Me); 25.86 (CH$_2$C$\underline{H}_2$CH$_2$); 32.63, 32.71 (C$\underline{H}_2$CH$_2$C$\underline{H}_2$); 42.17 (CH$_2$ of indene); 115.63 (=CH of indene); 119.52, 127.05 (CH arom.); 139.55, 141.71, 142.05, 144.36, 145.01 (C arom., =C$\underline{M}$e).

1-(Fluoren-9-yl)-2-(2-methyl-5,6-dihydrocyclopenta[*f*]-1*H*-inden-3-yl)ethane (1a) and 1-(fluoren-9-yl)-2-(2-methyl-5,6-dihydrocyclopenta[*f*]-1*H*-inden-1-yl)ethane (1b). Method *1*. A 2.5 *M* Bu^{n}Li solution in hexane (10.0 mL, 25.0 mmol) was added with stirring to a solution of indene **4** (3.63 g, 21.3 mmol) in THF (50 mL) at −20 °C for 15 min. The reaction mixture was warmed to ~20 °C and heated on a water bath at 55 °C for 20 min. Then a solution of tosylate **6** (7.30 g, 20.0 mmol) in THF (50 mL) was slowly (~4 h) added to the resulting lithium salt at ~20 °C. The reaction mixture was allowed to stand for ~18 h and heated at 60 °C for 30 min. The solvent was removed in vacuum created by a water-aspirator pump. The residue was dried under high vacuum and washed on a filter with benzene (3×50 mL). The extract (TLC data, benzene—light petroleum, 1 : 9) contained three compounds, including the starting indene **4**. The mixture was separated by column chromatography on silica gel (light petroleum as the eluent). The latter fraction was eluted from the column with benzene. The fraction *3* was concentrated, and the precipitate was washed on a filter with hexane and dried under high vacuum. The fraction *2* was concentrated, and the resulting compound was crystallized from hexane, twice washed on a filter with a minimum amount of cold hexane, and dried under high vacuum. The fraction *1* was worked up analogously.

Fraction *3* (compound **1a**). A white powdered compound, the yield was 1.87 g (26%). Found (%): C, 92.73; H, 7.20. $C_{28}H_{26}$. Calculated (%): C, 92.77; H, 7.23. ^1H NMR ($CDCl_3$, 25 °C), δ: 1.83 (s, 3 H, Me); 2.08 (m, 2 H, CH$_2$C$\underline{H}_2$CH$_2$ of indane); 2.11 and 2.30 (both m, 2 H each, bridging CH$_2$CH$_2$); 2.89 (m, 4 H, C$\underline{H}_2$CH$_2$C$\underline{H}_2$ of indane); 3.11 (s, 2 H, CH$_2$ of indene); 4.10 (t, 1 H, H(9) of fluorene, $^3J_{H,H}$ = 5.0 Hz); 6.91 and 7.17 (both s, 1 H each, H arom. of indene); 7.36 (m, 4 H, H(2), H(3), H(6), H(7) arom. of fluorene); 7.58 and 7.78 (both d, 2 H each, H(1), H(4), H(5), H(8) arom. of fluorene, $^3J_{H,H}$ = 7.1 Hz). $^{13}C\{^1H\}$ NMR ($CDCl_3$, 25 °C), δ: 13.78 (Me); 20.45, 31.19 (bridging CH$_2$CH$_2$); 25.92 (CH$_2$C$\underline{H}_2$CH$_2$ of indane); 32.64, 32.84 (C$\underline{H}_2$CH$_2$C$\underline{H}_2$ of indane); 41.98 (CH$_2$ of indene); 47.58 (CH(9) of fluorene); 113.96, 119.42 (CH arom. of indene); 119.87, 124.17, 126.93, 126.99 (CH arom. of fluorene); 136.72, 137.43, 139.54, 141.00, 141.77, 144.99 (=C, C arom. of indene); 141.41 (C(4a), C(4b) of fluorene); 147.01 (C(8a), C(9a) of fluorene).

Fraction *2* (spiro[fluorene-9,1′-cyclopropane] (**7**)). A crystalline snow-white compound, the yield was 0.93 g (24%).

^{1}H NMR ($CDCl_3$, 25 °C), δ: 1.72 (s, 4 H, CH_2); 7.05 and 7.83 (both d, 2 H each, H(1), H(4), H(5), H(8), $^3J_{H,H}$ = 7.4 Hz); 7.29 and 7.35 (both t, 2 H each, H(2), H(3), H(6), H(7), $^3J_{H,H}$ = 7.4 Hz). ^{13}C NMR ($CDCl_3$, 25 °C), δ: 18.30 (t, CH_2, $^1J_{C,H}$ = 164 Hz); 29.41 (s, C(9)); 118.57 (d, CH arom., $^1J_{C,H}$ = 156 Hz); 119.94 (d, CH arom., $^1J_{C,H}$ = 158 Hz); 125.93 and 126.75 (both d, CH arom., $^1J_{C,H}$ = 159 Hz); 139.81 and 148.07 (both s, C arom.).

Fraction *1* (starting indene **4**). The yield was 0.83 g (25%).

Method *2*. A solution of lithium salt **5**, which was prepared analogously to the method *1* from a solution of indene **4** (6.00 g, 35.2 mmol) in THF (80 mL), was slowly added to a solution of tosylate **6** (12.84 g, 35.2 mmol) in THF (80 mL) at ~20 °C for ~6 h. The reaction mixture was kept for ~18 h, quenched with a saturated aqueous solution of NH_4Cl (5 mL), and worked up analogously to the method *1*.

Fraction *3* (compound **1b**). A white powdered compound. The yield was 2.12 g (17%). Found (%): C, 92.70; H, 7.22. $C_{28}H_{26}$. Calculated (%): C, 92.77; H, 7.23. ^{1}H NMR ($CDCl_3$, 25 °C), δ: 1.39—1.79 (m, 4 H, bridging CH_2CH_2); 1.90 (s, 3 H, Me); 2.11 (m, 2 H, $CH_2C\underline{H}_2CH_2$ of indane); 2.91 (m, 4 H, $C\underline{H}_2CH_2C\underline{H}_2$ of indane); 3.07 (t, 1 H, $C\underline{H}CH_2$ of indene, $^3J_{H,H}$ = 4.5 Hz); 3.88 (t, 1 H, H(9) of fluorene, $^3J_{H,H}$ = 4.9 Hz); 6.41 (s, 1 H, =CH of indene); 6.99 and 7.08 (both s, 1 H, H arom. of indene); 7.28—7.40 (m, 5 H, H arom. of fluorene); 7.45 (d, 1 H, H arom. of fluorene, $^3J_{H,H}$ = 7.3 Hz); 7.76 (d, 2 H, H arom. of fluorene, $^3J_{H,H}$ = 7.4 Hz). ^{13}C NMR ($CDCl_3$, 25 °C), δ: 15.07 (q, Me, $^1J_{C,H}$ = 127 Hz); 23.74 and 25.85 (both t, bridging CH_2CH_2, $^1J_{C,H}$ = 122 Hz); 25.79 (t, $CH_2\underline{C}H_2CH_2$ of indane, $^1J_{C,H}$ = 127 Hz); 32.71 and 32.74 (both t, $\underline{C}H_2CH_2\underline{C}H_2$ of indane, $^1J_{C,H}$ = 130 Hz); 47.04 (d, CH(9) of fluorene, $^1J_{C,H}$ = 128 Hz); 50.96 (d, $\underline{C}HCH_2$ of indene, $^1J_{C,H}$ = 126 Hz); 115.57 (d, =CH of indene, $^1J_{C,H}$ = 157 Hz); 118.85, 119.70, 119.75, 124.05, 124.30, 126.74, 126.82, 126.86 (2 CH), and 127.03 (all d, CH arom., $^1J_{C,H}$ = 155—160 Hz); 139.63, 142.20, 143.65, 145.06, and 147.69 (all s, =$\underline{C}$Me and C arom. of indene); 141.31 (C(4a), C(4b) of fluorene); 146.89, 147.11 (C(8a), C(9a) of fluorene).

Fraction *2* (compound **7**). The yield was 4.34 g (64%).

Fraction *1* (starting indene **4**). The yield was 3.75 g (63%).

Dilithium derivative of 1-(fluoren-9-yl)-2-(2-methyl-5,6-dihydrocyclopenta[*f*]-1*H*-inden-1-yl)ethane (8). The synthesis was carried out in all-sealed evacuated vessels. A 2.7 *M* Bu^{n}Li solution in hexane (7.0 mL, 18.9 mmol) was added portionwise with vigorous stirring to a suspension of compound **1b** (3.00 g, 8.3 mmol) in Et_2O (80 mL) at −20 °C for 5 min. The reaction mixture was allowed to warm to ~20 °C and kept for ~18 h. The solvent was distilled off to a liquid nitrogen cooled tube. The residue was twice washed on a porous glass membrane with a 4 : 1 Et_2O—hexane mixture (100 mL) and then with pure hexane (50 mL) and dried under high vacuum. An orange-brown powdered compound was obtained in a yield of 3.00 g (91%). There are four molecules of dilithium salt **8** per Et_2O molecule (^{1}H NMR spectroscopic data). ^{1}H NMR (THF-d_8, 25 °C), δ: 2.09 (m, 2 H, $CH_2C\underline{H}_2CH_2$ of indane); 2.51 (s, 3 H, Me); 2.93 and 3.00 (both m, 2 H each, $C\underline{H}_2CH_2C\underline{H}_2$ of indane); 3.09 and 3.24 (both m, 2 H each, bridging CH_2CH_2); 5.61 (s, 1 H, H arom. of C(5)-indene); 6.37 and 6.86 (both br.t, 2 H each, H(2), H(3), H(6), H(7) of fluorene); 7.09 and 7.47 (both s, 1 H each, H arom. of C(6)-indene); 7.52 and 7.88 (both br.d, 2 H each, H(1), H(4), H(5), H(8) of fluorene). ^{13}C NMR (THF-d_8, 25 °C), δ: 14.94 (q, Me, $^1J_{C,H}$ = 124 Hz); 28.23 (t, $CH_2\underline{C}H_2CH_2$ of indane, $^1J_{C,H}$ = 128 Hz); 29.56 and 31.57 (both t, bridging CH_2CH_2, $^1J_{C,H}$ = 120 Hz); 33.82 and 33.98 (both t, $\underline{C}H_2CH_2\underline{C}H_2$ of indane, $^1J_{C,H}$ = 128 Hz); 88.72 (d, CH arom. of C(5)-indene, $^1J_{C,H}$ = 160 Hz); 95.94 (s, C(9) of fluorene); 106.72 (s, $\underline{C}CH_2$ of C(5)-indene); 107.09, 114.33, 118.78, and 118.81 (all d, C(1)—C(8) of fluorene, $^1J_{C,H}$ = 149—153 Hz); 112.65 and 113.36 (both d, CH arom. of C(6)-indene, $^1J_{C,H}$ = 149 Hz); 122.23 and 135.65 (both s, C(4a), C(4b), C(8a), C(9a) of fluorene); 124.04 (s, $\underline{C}$Me of C(5)-indene); 126.82 (2 C), 129.22, and 129.86 (all s, C arom. of C(6)-indene).

The reaction with compound **1a** was carried out analogously.

***rac*-{1-(η^5-Fluoren-9-yl)-2-(2-methyl-5,6-dihydrocyclopenta[*f*]-η^5-inden-1-yl)ethane}zirconium dichloride (9).** The synthesis was carried out in all-sealed evacuated vessels. Zirconium chloride $ZrCl_4$ (1.18 g, 5.1 mmol) was added to a suspension of salt **8** (2.00 g, 5.1 mmol) in toluene (100 mL) at −30 °C. The reaction mixture was allowed to warm to ~20 °C (the precipitate was virtually completely dissolved), stirred at ~20 °C for 15 h, heated at 95 °C for 4 h, cooled to ~20 °C, and allowed to stand for ~18 h. The solution was decanted and the residue was extracted with toluene (2×100 mL). The extract was concentrated to ~15 mL with heating and then cooled to 0 °C. The crystals that precipitated were separated from the mother liquor, twice washed with a minimum amount of cold toluene and then with Et_2O (2×30 mL), and dried under high vacuum. An orange-red crystalline compound was obtained in a yield of 1.38 g (2.6 mmol). The mother liquor was again worked up to obtain an additional amount of the product (0.24 g, 0.5 mmol). The total yield was 1.62 g (61%). Found (%): C, 64.28; H, 4.59. $C_{28}H_{24}Cl_2Zr$. Calculated (%): C, 64.35; H, 4.63. ^{1}H NMR (CD_2Cl_2, 25 °C), δ: 1.96—2.06 (m, 2 H, $CH_2C\underline{H}_2CH_2$ of indane); 2.15 (s, 3 H, Me); 2.82—3.00 (m, 4 H, $C\underline{H}_2CH_2C\underline{H}_2$ of indane); 3.81 and 4.14 (both m, 1 H each, bridging CH_2); 4.02 and 4.66 (both m, 1 H each, bridging CH_2); 6.04 (s, 1 H, H arom. of C(5)-indene); 7.08 and 7.78 (both s, 1 H each, H arom. of C(6)-indene); 7.09, 7.26, 7.38, and 7.57 (all t, 1 H each, H(2), H(3), H(6), H(7) of fluorene, $^3J_{H,H} \approx$ 8.0 Hz); 7.53, 7.73, 7.87, and 7.88 (all d, 1 H each, H(1), H(4), H(5), H(8) of fluorene, $^3J_{H,H} \approx$ 8.0 Hz). ^{13}C{^{1}H} NMR (CD_2Cl_2, 25 °C), δ: 15.44 (Me); 26.50, 28.68, 30.23, 32.60, 32.88 (CH_2 of the bridge and indane); 107.43 (CH arom. of C(5)-indene); 116.72, 119.52, 122.84, 124.11, 124.37, 124.66, 125.16, 125.89, 127.74, 128.46 (CH arom. of C(6)-indene and fluorene); 103.93, 121.67, 123.54, 123.58, 126.71, 128.51, 130.48, 131.84, 143.54, 145.05 (2 C) (C arom.).

***rac*-{1-(η^5-Fluoren-9-yl)-2-(2-methyl-5,6-dihydrocyclopenta[*f*]-η^5-inden-1-yl)ethane}hafnium dichloride (10).** The synthesis was carried out analogously to the synthesis of zirconium complex **9** starting from salt **8** (0.95 g, 2.46 mmol) and $HfCl_4$ (0.79 g, 2.46 mmol). A yellow crystalline compound was obtained in a yield of 1.18 g (78%). Found (%): C, 55.05; H, 3.89. $C_{28}H_{24}Cl_2Hf$. Calculated (%): C, 55.14; H, 3.97. ^{1}H NMR (CD_2Cl_2, 25 °C), δ: 1.94—2.06 (m, 2 H, $CH_2C\underline{H}_2CH_2$ of indane); 2.23 (s, 3 H, Me); 2.84—3.03 (m, 4 H, $C\underline{H}_2CH_2C\underline{H}_2$ of indane); 3.94 and 4.10 (both m, 1 H each, bridging CH_2); 4.21 and 4.61 (both m, 1 H each, bridging CH_2); 5.92 (s, 1 H, H arom. of C(5)-indene); 7.09 and 7.75 (both s, 1 H each, H arom. of C(6)-indene); 7.03, 7.23, 7.33, and 7.48 (all t, 1 H each, H(2), H(3), H(6), H(7) of fluorene, $^3J_{H,H} \approx$ 8.0 Hz); 7.48, 7.74, 7.86, and 7.88 (all d, 1 H each, H(1), H(4), H(5), H(8) of fluorene, $^3J_{H,H} \approx$ 8.0 Hz). ^{13}C{^{1}H} NMR (CD_2Cl_2, 25 °C), δ: 15.20 (Me);

26.59, 27.94, 29.44, 32.52, 32.79 (CH_2 of bridge and indane); 104.66 (CH arom. of C(5)-indene); 116.66, 119.26, 122.63, 123.96, 124.22, 124.34, 125.06, 125.60, 127.44, 128.26 (CH arom. of C(6)-indene and fluorene); 99.54, 119.03, 121.90, 123.89, 126.24, 127.79, 129.91, 130.10, 143.08, 144.92 (2 C) (C arom.).

X-ray diffraction study of compounds 1b (two modifications) and 10. The structures were solved by direct methods using the SHELX-86 program package.[32] All nonhydrogen atoms were refined anisotropically by the full-matrix least-squares method against F^2 (SHELXL-97).[33] For the monoclinic modification of **1b** and for compound **10**, all H atoms were located from difference electron density series and refined isotropically. In the structure of the orthorhombic modification of **1b**, all H atoms were placed in calculated positions and refined using a riding model. The crystallographic data, details of X-ray diffraction data collection, and characteristics of structure refinement for **1b** ($P2_1/c$), **1b** (*Pbca*), and **10** are given in Table 8. Complete tables of atomic coordinates, bond angles, and bond angles were deposited with the Cambridge Structural Database.

Polymerization. Polymethylalumoxane (Witco; a 10% solution in toluene) and triisobutylaluminum (Aldrich) were used without additional purification. The kinetics of propene polymerization was studied on an apparatus equipped with a 0.4-L autoclave-type reactor. The apparatus was evacuated at 60—70 °C for 1 h. Then MAO or TIBA was supplied to the reactor filled with the liquid monomer, after which a solution of metallocene in MAO was added (at the polymerization temperature). Polymerization was carried out at a constant pressure of the monomer in the mode of complete filling of the reactor with the liquefied monomer in the temperature range of 30—70 °C. The polymerization rate was calculated from the amount of the propene consumed, which was determined using a calibration syringe. The activity of the systems under study was characterized by the effective polymerization rate constant

$$k_{eff} = W_p \cdot C_m^{-1} \cdot C_M^{-1},$$

where W_p/mol L^{-1} min^{-1} is the propene polymerization rate at a particular instant of time in the unit volume of the reaction

Table 8. Crystallographic data, details of X-ray diffraction study, and characteristics of structure refinement of **1b** ($P2_1/c$), **1b** (*Pbca*), and **10**

Parameter	**1b**	**1b**	**10**
Molecular formula	$C_{28}H_{26}$	$C_{28}H_{26}$	$C_{28}H_{26}Cl_2Hf$
Molecular weight	362.49	362.49	609.86
Crystal system	Monoclinic	Orthorhombic	Triclinic
Space group	$P2_1/c$	*Pbca*	$P\bar{1}$
a/Å	9.5443(4)	19.978(4)	7.854(4)
b/Å	8.2592(3)	16.311(4)	10.861(5)
c/Å	25.949(1)	25.705(9)	14.410(1)
α/deg	—	—	70.91(5)
β/deg	95.694(2)	—	75.24(5)
γ/deg	—	—	79.57(4)
V/Å^3	2035.4(1)	8376(4)	1116.8(8)
Z	4	16	2
d_{calc}/g cm^{-3}	1.183	1.150	1.814
F(000)	776	3104	596
μ(Mo-Kα)/mm^{-1}	0.066	0.065	4.923
Diffractometer	«Bruker SMART»	«Enraf-Nonius CAD4»	
T/K	100	293	293
Scan mode	ω	ω	ω
θ Scan range/deg	1.58—28.00	2.04—24.98	2.13—24.97
Ranges of indices of measured reflections	$-12 \le h \le 12$, $-10 \le k \le 10$, $-31 \le l \le 34$	$0 \le h \le 23$, $0 \le k \le 19$, $-30 \le l \le 0$	$-9 \le h \le 9$, $-11 \le k \le 12$, $-3 \le l \le 17$
Number of measured reflections	13115	7347	5070
Number of independent reflections	4910 (R_{int} = 0.0767)	7347 (R_{int} = 0.0000)	3898 (R_{int} = 0.0220)
Absorption correction	—	—	ψ Scan
Transmission (min/max)	—	—	0.27464/0.42504
Number of parameters in refinement	358	508	377
R factor using reflections with $I > 2\sigma(I)$	R_1 = 0.0576, wR_2 = 0.1511	R_1 = 0.0606, wR_2 = 0.1122	R_1 = 0.0172, wR_2 = 0.0407
Goodness-of-fit on F^2	1.013	0.816	1.055
Extinction coefficient	0.0010(9)	0.00031(5)	0.0022(2)
Residual electron density (min/max)/e Å^{-3}	−0.346/0.463	−0.203/0.184	−0.533/0.694

mixture, C_m/mol L^{-1} is the concentration of the monomer in the liquid phase, and C_M/mol L^{-1} is the concentration of metallocene in the unit volume of the reaction mixture.

Study of the properties of polymers. The microstructures of PP samples were determined by IR and ^{13}C NMR spectroscopy. The stereoregularity parameters were determined from the intensity ratio of the absorption bands D_{998}/D_{973} (macrotacticity) according to a known procedure.[34] The ^{13}C NMR spectra of polymer solutions in 1,2-$C_2D_2Cl_4$ (5—10 wt.%) were recorded on a Bruker AC-200 instrument at 110 °C.

The molecular-weight characteristics of PP were determined on a Waters 150-C gel chromatograph at 145 °C in *o*-dichlorobenzene with the use of an HT-μ-styragel linear column calibrated with polystyrene.

The melting point of PP was determined by the DSC method on a DuPont Instrument at a heating and cooling rate of 10 °C min^{-1}.

X-ray diffraction measurements were carried out on a DRON-3M diffractometer in the transmission mode (asymmetric, focusing on the detector, a quartz primary beam monochromator) using Cu-Kα radiation. The X-ray diffraction patterns were scanned in the diffraction angle range $2\theta = 6—36°$ with a step $\Delta 2\theta = 0.04°$ and the accumulation time $\tau = 10$ s. The X-ray diffraction patterns were processed using the Peak Fit ver. 4.0 program package. To separate scattering from the amorphous and crystalline components in the X-ray patterns of PP, a completely amorphous PP sample was used (see Table 3, run *1*).

Samples for physicochemical tests were prepared by pressing at 190 °C. Irganox (~0.8 wt.%) was introduced into the polymer as the stabilizer. The tensile tests were carried out on an Instron 1122 instrument on blade-shaped samples (the cross-section was 1.5×5 mm, and the base length was 35 mm) in the following mode: (1) stretching by 300% at a rate of 500 mm min^{-1}; (2) traverse at a rate of 500 mm min^{-1} to the zero tension; (3) repeated stretching of the sample at a rate of 500 mm min^{-1} until rupture occurred. The elasticity of the polymers was estimated using the residual strain (ε_{300}) or the residual stress (ε_{res}) expressed in % and determined from the equation:

$$\varepsilon = (L_1 - L_0) \cdot L_0^{-1} \cdot 100,$$

where L_1 is the final length of the sample after removal of loading as the stretching became as large as 300% or after rupture, and L_0 is the initial length of the sample.

We thank L. G. Echevskaya and M. A. Matsko for measuring the molecular-weight characteristics of polypropylene samples. We also acknowledge A. N. Shchegolikhin for performing DSC and IR analyses of these samples.

This study was financially supported by the Russian Foundation for Basic Research (Project No. 03-03-32566) and the Foundation of the President of the Russian Federation (Program for Support of Young Doctors, Grant MK-3697.2004.3).

References

1. H.-H. Brintzinger, D. Fischer, and R. Mulhaupt, *Angew. Chem., Int. Ed. Engl.*, 1995, **34**, 1143.
2. *Metallocene-Based Polyolefins: Preparation, Properties and Technology*, Eds J. Scheirs and W. Kaminsky, Wiley, New York, 2000, **1**, **2**.
3. W. Kaminsky, *J. Chem. Soc., Dalton Trans.*, 1998, **9**, 1413.
4. V. I. Tsvetkova, *Vysokomol. Soedin., Ser. C*, 2000, **42**, 1954 [*Polym. Sci., Ser. C*, 2000, **42** (Engl. Transl.)].
5. G. Natta, G. Mazzanti, G. Crespi, and G. Moraglio, *Chim. Ind. Milan*, 1957, **39**, 275.
6. G. W. Coates and R. M. Waymouth, *Science*, 1995, **267**, 217.
7. N. M. Bravaya, P. M. Nedorezova, and V. I. Tsvetkova, *Usp. Khim.*, 002, **71**, 57 [*Russ. Chem. Rev.*, 2002, **71**, 49 (Engl. Transl.)].
8. S. Lieber and H.-H. Brintzinger, *Macromolecules*, 2000, **33**, 9192.
9. J. C. W. Chien, Y. Iwamoto, and M. D. Rausch, *J. Polym. Sci., Part A*, 1999, **37**, 2439.
10. J. C. W. Chien, G. H. Llinas, and M. D. Rausch, *J. Polym. Sci., Part A*, 1992, **30**, 2601.
11. W. J. Gautier, J. F. Corrigan, N. J. Taylor, and S. Collins, *Macromolecules*, 1995, **28**, 3771.
12. J. Kukral and B. Rieger, *Macromol. Symp.*, 2002, **177**, 71.
13. B. Rieger, C. Troll, and J. Preuschen, *Macromolecules*, 2002, **35**, 5742.
14. G. Guerra, L. Cavallo, G. Moscardi, M. Vacatello, and P. Corradini, *Macromolecules*, 1996, **29**, 4834.
15. U. Dietrich, M. Hackmann, B. Rieger, M. Klinga, and M. Leskel, *J. Am. Chem. Soc.*, 1999, **121**, 4348.
16. F. H. Allen, O. Kennard, D. G. Watson, L. Brammer, A. G. Orpen, and R. Taylor, *J. Chem. Soc., Perkin Trans. 2*, 1987, 1.
17. D. J. Cardin, M. F. Lappert, C. L. Raston, and P. I. Riley, in *Comprehensive Organometallic Chemistry*, Eds G. Wilkinson, F. Gordon, A. Stone, and E. W. Abel, Pergamon Press, Oxford—New York—Toronto—Sydney—Paris—Frankfurt, 1982, **3**, 551.
18. A. Razavi, L. Peters, L. Nafpliotis, D. Vereecke, K. D. Dauw, J. L. Atwood, and U. Thewald, *Macromol. Symp.*, 1995, **89**, 345.
19. C. W. Chien and B. P. Wang, *J. Polym. Sci., Part A*, 1989, **27**, 1539.
20. F. Auriemma and C. De Rosa, *Macromolecules*, 2002, **35**, 9057.
21. V. Busico, L. Caporaso, R. Cipullo, and L. Landriani, *J. Am. Chem. Soc.*, 1996, **118**, 2105.
22. A. N. Panin, Z. M. Dzhabieva, P. M. Nedorezova, V. I. Tsvetkova, S. L. Saratovskikh, O. N. Babkina, and N. M. Bravaya, *J. Polym. Sci., Part A*, 2001, **39**, 1915.
23. O. N. Babkina, N. M. Bravaya, P. M. Nedorezova, S. L. Saratovskikh, and V. I. Tsvetkova, *Kinet. Katal.*, 2002, **43**, 371 [*Kinet. Catal.*, 2002, **43**, 341 (Engl. Transl.)].
24. P. M. Nedorezova, V. I. Tsvetkova, A. M. Aladyshev, D. V. Savinov, A. N. Klyamkina, V. A. Optov, and D. A. *Vysokomol. Soedin., Ser. A*, 2001, **43**, 595 [*Polym. Sci., Ser. A*, 2001, **43**, 356 (Engl. Transl.)].
25. P. M. Nedorezova, A. M. Aladyshev, D. V. Savinov, E. N. Veksler, V. I. Tsvetkova, and D. A. Lemenovskii, *Kinet. Katal.*, 2003, **44**, 341 [*Kinet. Catal.*, 2003, **44**, 320 (Engl. Transl.)].

26. R. Thomann, H. Semke, R. D. Maier, Y. Thomann, J. Scherble, R. Mulhaupt, and J. Oressler, *Polymer*, 2001, **42**, 4597.
27. S. V. Meille, S. Bruckner, and W. Porzio, *Macromolecules*, 1990, **23**, 4114.
28. B. F. Shklyaruk, V. E. Dreval´, V. A. Bocharova, V. G. Kulichikhin, V. N. Kuleznev, and E. M. Antipov, *Vysokomol. Soedin., Ser. A*, 2004, **46**, 1 [*Polym. Sci., Ser. A*, 2004, **46** (Engl. Transl.)].
29. D. D. Perrin, W. L. F. Armarego, and D. N. Perrin, *Purification of Laboratory Chemicals*, Pergamon Press, Oxford, 1966, 362 pp.
30. B. Rieger, G. Jany, R. Fawzi, and M. Steiman, *Organometallics*, 1994, **13**, 647.
31. R. S. Tipson and L. H. Cretcher, *J. Am. Chem. Soc.*, 1942, **64**, 1162.
32. G. M. Sheldrick, *Acta Crystallogr., Sect. A*, 1990, **46**, 467.
33. G. M. Sheldrick, *SHELXL-97. Program for the Refinement of Crystal Structures*, University of Göttingen, Göttingen (Germany), 1997.
34. Yu. V. Kissin, *Isospecific Polymerization of Olefins*, Springer-Verlag, New York—Berlin—Heidelberg—Tokyo, 1985.

Received May 21, 2004;
in revised form October 18, 2004